

## REPORT

## IMMUNOLOGY

## Structural insights into immunoglobulin M

Yaxin Li<sup>1,2\*</sup>, Guopeng Wang<sup>3\*</sup>, Ningning Li<sup>2,3</sup>, Yuxin Wang<sup>1,2</sup>, Qinyu Zhu<sup>1,2</sup>, Huarui Chu<sup>1,2</sup>, Wenjun Wu<sup>4,5</sup>, Ying Tan<sup>4,5</sup>, Feng Yu<sup>4,5,6</sup>, Xiao-Dong Su<sup>1</sup>, Ning Gao<sup>2,3</sup>, Junyu Xiao<sup>1,2†</sup>

Immunoglobulin M (IgM) plays a pivotal role in both humoral and mucosal immunity. Its assembly and transport depend on the joining chain (J-chain) and the polymeric immunoglobulin receptor (pIgR), but the underlying molecular mechanisms of these processes are unclear. We report a cryo-electron microscopy structure of the Fc region of human IgM in complex with the J-chain and pIgR ectodomain. The IgM-Fc pentamer is formed asymmetrically, resembling a hexagon with a missing triangle. The tailpieces of IgM-Fc pack into an amyloid-like structure to stabilize the pentamer. The J-chain caps the tailpiece assembly and bridges the interaction between IgM-Fc and the polymeric immunoglobulin receptor, which undergoes a large conformational change to engage the IgM-J complex. These results provide a structural basis for the function of IgM.

Immunoglobulin M (IgM) is the first class of antibody produced after B cell activation. Secretory IgM, together with IgA, plays a critical role in the mucosal immune system.

IgM forms oligomers, and the presence of multivalent antigen-binding sites in IgM oligomers is a key factor in their ability to agglutinate pathogens. The heavy chain of IgM contains a C-terminal extension known as the tailpiece that is essential for oligomerization. In the presence of the joining chain (J-chain), a 15-kDa protein that has no homology to other proteins, IgM forms a pentamer, in which five IgM monomers are linked by disulfide bonds between each other and with the J-chain (1–3). The J-chain also facilitates the dimerization of IgA, which contains a similar tailpiece. The overall structural organization of the IgM pentamer is not completely understood, nor is the function of the J-chain in regulating the assembly processes of these polymeric immunoglobulins.

Furthermore, to function at the mucosal surface, IgM secreted by the plasma cells must be transcytosed through the mucosal epithelial cells. This process critically depends on the polymeric immunoglobulin receptor (pIgR) (4, 5). pIgR is a type I transmembrane protein that contains five extracellular immunoglobulin-like domains (D1 to D5). It specifically binds to J-chain-containing secretory IgM and IgA at the

basolateral surface of epithelial cells and escorts them to the apical side. There, the ectodomain is released by proteolysis and secreted together with IgM and IgA. The free ectodomain is often referred to as the secretory component (SC). The molecular mechanism of how pIgR/SC facilitates the secretion of IgM and IgA also remains elusive.

To gain insight into the assembly and secretion of IgM, we reconstituted a tripartite complex containing the Fc region of human IgM (Fc<sub>μ</sub>), J-chain, and SC (fig. S1), which was then analyzed using cryo-electron microscopy (cryo-EM) (fig. S2). The final constructed model reveals that an IgM C<sub>μ</sub>3–C<sub>μ</sub>4-tailpiece pentamer and a J-chain molecule form a near-planar structure, and a triangular SC docks perpendicularly to the Fc<sub>μ</sub>-J plane (Fig. 1). The center region of the structure, including the IgM-C<sub>μ</sub>4 domains and tailpieces, the J-chain, and the D1 domain of pIgR/SC, displayed better than 3 Å resolution, with most of the side chains clearly visualizable (figs. S2 and S3).

Although the structures of individual mouse IgM-C<sub>μ</sub>2, IgM-C<sub>μ</sub>3, and IgM-C<sub>μ</sub>4 domains have been previously characterized (6), the structure of an entire Fc<sub>μ</sub> has yet to be elucidated. In our structure, IgM-C<sub>μ</sub>4 forms a dimer within each Fc<sub>μ</sub> monomer (fig. S4A). The IgM-C<sub>μ</sub>4 dimer here highly resembles the dimers formed by IgA-C<sub>α</sub>3, IgG-C<sub>γ</sub>3, and IgE-C<sub>ε</sub>4, but is remarkably distinct from the “parallel” dimer observed in the mouse IgM-C<sub>μ</sub>4 crystal structure (fig. S4). The IgM-C<sub>μ</sub>4 dimer here buries 2540 Å<sup>2</sup> of surface area, larger than the 1900-Å<sup>2</sup> surface concealed by the mouse IgM-C<sub>μ</sub>4 dimer. The physiological importance of these different IgM-C<sub>μ</sub>4 dimers remains unclear. The IgM-C<sub>μ</sub>3 domains are not involved in direct contacts within each Fc<sub>μ</sub> monomer (fig. S4A). In some determined structures of IgE, the IgE-C<sub>ε</sub>2 dimer bends acutely and packs against IgE-C<sub>ε</sub>3 and

IgE-C<sub>ε</sub>4 (fig. S4E). On the basis of homology modeling, the IgM-C<sub>μ</sub>2 dimer was thought to bend similarly (7). However, the densities corresponding to the IgM-C<sub>μ</sub>2 dimers, albeit weak, suggest that they do not adopt a stably bent conformation (fig. S4F).

IgM forms a pentamer in the presence of the J-chain. Earlier EM studies depicted a stellate appearance of the IgM pentamer with a five-fold symmetry (8). Although this model is widely documented in textbooks, a recent negative-stain EM study shows that the IgM pentamer is an asymmetric pentagon with a 50° gap (9). A similar gap is present in our structure and is occupied by the J-chain (Fig. 2A). Nonetheless, the gap in our structure has a 61° angle, and the five Fc<sub>μ</sub> units are arranged in an almost perfect hexagonal symmetry. We speculate that if the J-chain was not present, a sixth Fc<sub>μ</sub> unit could be readily accommodated to form a hexamer. This is consistent with a recent electron tomography study showing that the IgM pentamer is equivalent to the hexamer except for the J-chain (10). IgM-C<sub>μ</sub>3 and IgM-C<sub>μ</sub>4 as well as the tailpieces all contribute to pentamer formation (Fig. 2A). Cys<sup>414</sup> residues from two neighboring IgM-C<sub>μ</sub>3 domains are adjacent to one another and likely form interchain disulfide bonds, consistent with earlier analyses (11). The FG loops mediate the interaction between two neighboring IgM-C<sub>μ</sub>4 domains. The seven residues Tyr<sup>562</sup> to Met<sup>568</sup> in each tailpiece form a β strand, and the 10 strands are arranged into two five-stranded parallel β sheets that pack onto one another in an antiparallel fashion. This is reminiscent of the cross-β fibers seen in amyloid proteins and peptides (12) and provides the most prominent interactions to stabilize the IgM pentamer. The Tyr<sup>562</sup>, Val<sup>564</sup>, Leu<sup>566</sup>, and Met<sup>568</sup> side chains face inward and mediate hydrophobic interactions between the two sheets (Fig. 2B and fig. S3A). Mutation of each of these residues either abolished or significantly reduced the oligomerization of mouse IgM (13). Val<sup>567</sup> residues also stack onto one another to mediate packing interactions between adjacent strands, and mutation of the corresponding Ile<sup>567</sup> in mouse IgM disrupted its oligomerization (13). Notably, Val<sup>567</sup> residues are exposed to the solvent and form extended hydrophobic surface patches (Fig. 2B). The highly conserved Asn<sup>563</sup> and Ser<sup>565</sup> residues conform to the N-linked glycosylation consensus motif and facilitate the attachment of glycans on Asn<sup>563</sup> (Fig. 2B and fig. S3A), which is likely necessary to prevent IgM from forming aggregations. Cys<sup>575</sup>, the penultimate Cys, mediates the formation of disulfide bonds between adjacent Fc<sub>μ</sub> monomers, which is a prerequisite for IgM oligomerization (13, 14). Indeed, the Cys<sup>575</sup> residues of Fc<sub>μ</sub>5A and Fc<sub>μ</sub>4B are adjacent to one another and likely form a disulfide bond (Fig. 3A and fig. S3C). By contrast, Cys<sup>575</sup> of Fc<sub>μ</sub>5B and Cys<sup>575</sup> of Fc<sub>μ</sub>1A are linked to the J-chain.

<sup>1</sup>State Key Laboratory of Protein and Plant Gene Research, School of Life Sciences, Peking University, Beijing, China. <sup>2</sup>Peking-Tsinghua Center for Life Sciences, Peking University, Beijing, China. <sup>3</sup>State Key Laboratory of Membrane Biology, School of Life Sciences, Peking University, Beijing, China. <sup>4</sup>Renal Division, Department of Medicine, Peking University First Hospital, Beijing, China. <sup>5</sup>Institute of Nephrology, Peking University, Beijing, China. <sup>6</sup>Department of Nephrology, Peking University International Hospital, Beijing, China.

\*These authors contributed equally to this work.

†Corresponding author. Email: junyuxiao@pku.edu.cn

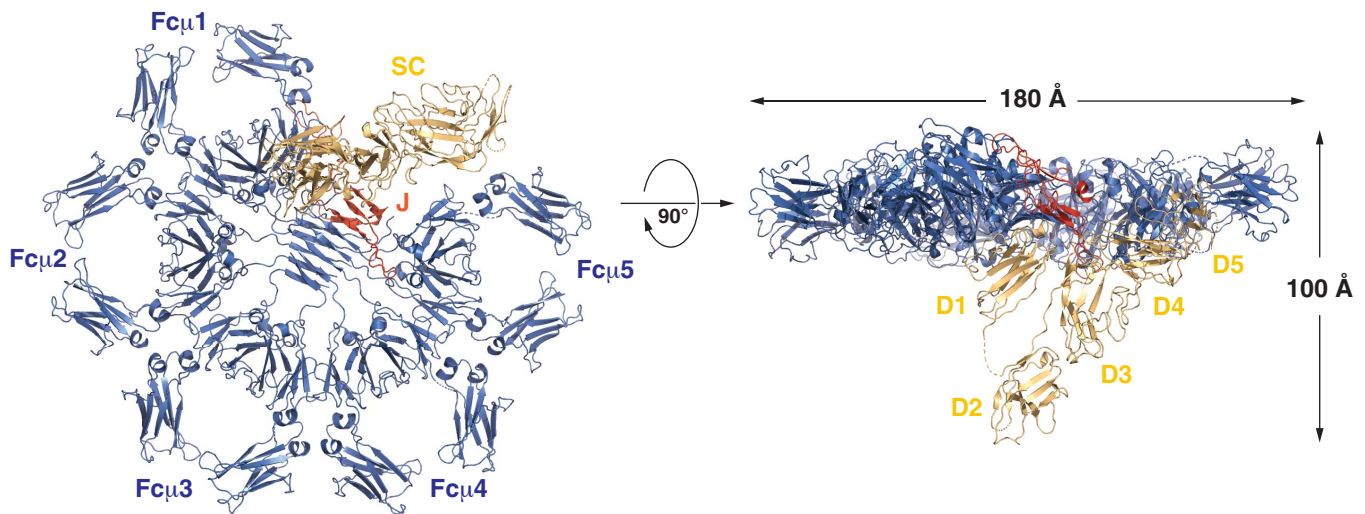


**Fig. 1. The cryo-EM structure of the Fc $\mu$  pentamer in complex with the J-chain and SC.** The five Fc $\mu$  monomers are shown in blue and labeled Fc $\mu$ 1 to Fc $\mu$ 5. The J-chain and SC are shown in red and gold, respectively.

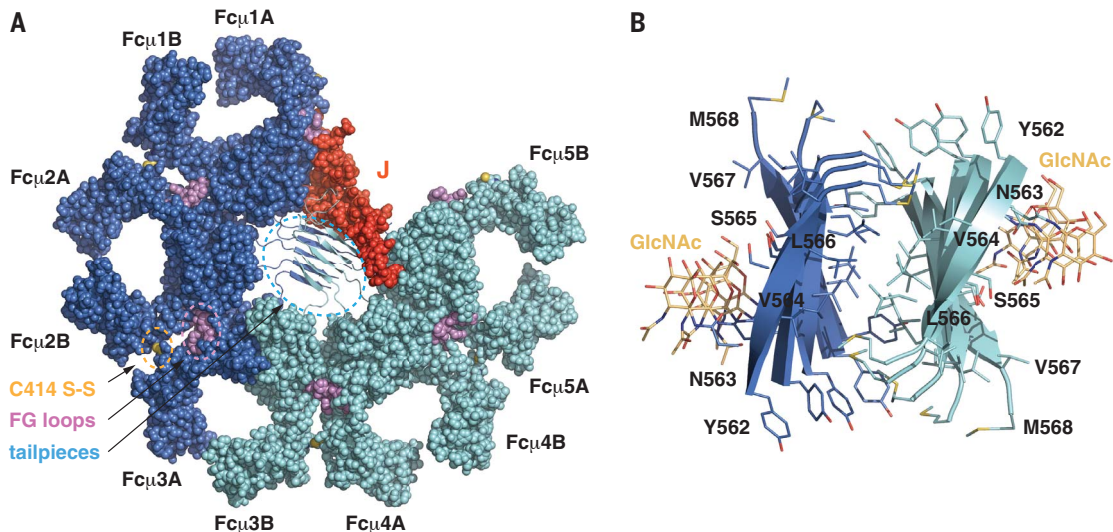


**Fig. 2. The Fc $\mu$  pentamer.** (A) The Fc $\mu$  pentamer is shown as a space-filling model except for the tailpieces, which are shown as ribbon diagrams. Five Fc $\mu$  chains are shown in blue and five are shown in cyan. The Cys<sup>414</sup> disulfide bonds and the FG loops are highlighted. (B) Detailed view of the tailpiece assembly. The *N*-acetylglucosamine (GlcNAc) molecules attached to Asn<sup>563</sup> are shown as orange sticks. Amino acid abbreviations in this or later figures: A, Ala; C, Cys; E, Glu; F, Phe; H, His; L, Leu; M, Met; N, Asn; P, Pro; Q, Gln; R, Arg; S, Ser; T, Thr; V, Val; Y, Tyr.

The J-chain was identified almost 50 years ago as an integral subunit of secretory IgA and IgM (15, 16). Guided by the disulfide bond assignments from earlier biochemical studies (17), we were able to build an atomic model for the majority of this protein (Fig. 3A and fig. S3B). It interacts with both Fc $\mu$ 1 and Fc $\mu$ 5 to seal the Fc $\mu$  pentamer. The N-terminal wing comprises four  $\beta$  strands ( $\beta$ 1 to  $\beta$ 4) and a short helix. The  $\beta$ 3 and  $\beta$ 4 strands pack on the tailpieces of Fc $\mu$ 5B and Fc $\mu$ 1A, respectively, to cap the fiber-like assembly of the IgM tailpieces. J-chain residue Cys<sup>14</sup> at the beginning of  $\beta$ 2 forms a disulfide bond with Cys<sup>575</sup> of Fc $\mu$ 5B, and J-chain residue

Cys<sup>68</sup> in the short helix forms a bond with Cys<sup>575</sup> of Fc $\mu$ 1A (Fig. 3A and fig. S3, D and E). The  $\beta$ 2- $\beta$ 3 loop interacts with the base of Fc $\mu$ 5B. The C-terminal wing contains a long hairpin-like structure, which reaches up to the C $\mu$ 3-C $\mu$ 4 junction of Fc $\mu$ 1A and makes extensive hydrophobic contacts (Fig. 3B and fig. S3, F to H). J-chain residues Val<sup>113</sup> and Pro<sup>114</sup> interact with Met<sup>489</sup>, Pro<sup>494</sup>, and Val<sup>537</sup> of Fc $\mu$ 1A, whereas J-chain residues Leu<sup>115</sup>, Val<sup>124</sup>, and Thr<sup>126</sup> interact with Phe<sup>358</sup>, Leu<sup>359</sup>, Phe<sup>485</sup>, and Val<sup>547</sup> of Fc $\mu$ 1A. J-chain residues Ala<sup>127</sup>, Pro<sup>130</sup>, and Tyr<sup>134</sup> form a pocket to accommodate Pro<sup>544</sup> of Fc $\mu$ 1A. Furthermore, this C-terminal hairpin

also interacts with pIgR/SC to connect IgM with the receptor.

pIgR/SC binds selectively to IgA or IgM that contains the J-chain (18). The D1 domain is the major binding site, and the three loops that are analogous to the complementarity-determining regions (CDRs) of immunoglobulin variable domains are all involved (Fig. 4A) (19–22). In the ligand-free state of pIgR/SC, D1 to D5 are arranged in the form of an isosceles triangle (22), with the D2-D3 and D4-D5 sides having similar lengths (Fig. 4B). In the Fc $\mu$ -J-SC complex, the D2-D3 side remains unaltered, whereas D1 and D4-D5 undergo drastic conformational

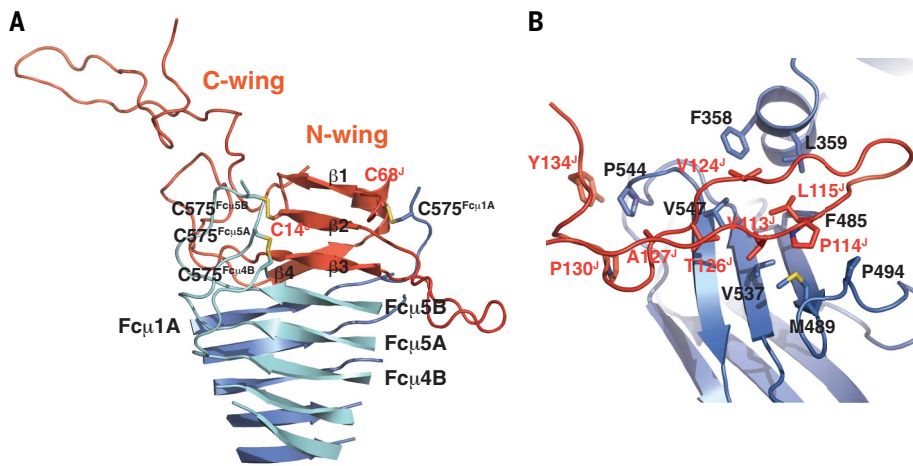


**Fig. 3. Structure of the J-chain and its interactions with Fc $\mu$ .** (A) The J-chain has a two-winged structure and interacts with the tailpieces of the Fc $\mu$  pentamer. (B) The C-terminal hairpin of the J-chain interacts with Fc $\mu$ 1A.

changes, leading to the formation of a very different triangular shape (Fig. 4C). D4-D5 rotates 120° en bloc to become co-linear with D2-D3, and the newly formed D3-D4 interface buries a large surface area (1486 Å<sup>2</sup>). D1 is rotated 84° and packs onto D2-D3. This large conformational change is consistent with a previous double electron-electron resonance (DEER) spectroscopy study (22). In particular, the distance between the C $\alpha$  atoms of D1-Thr<sup>67</sup> and D5-Gln<sup>491</sup> is 78 Å in this new conformation, in good agreement with DEER measurements showing that ligand binding induces a separation of these two residues beyond 70 Å. The three CDRs function as a central hub to mediate a network of interactions with Fc $\mu$ 1, Fc $\mu$ 5, and the J-chain (Fig. 4, A, D, and E, and fig. S3, I to N). In CDR1, pIgR/SC residue Val<sup>29</sup> interacts with J-chain residue Ala<sup>132</sup> in the J-chain C-terminal hairpin (Fig. 4D). pIgR/SC residue Asn<sup>30</sup> forms a hydrogen bond with

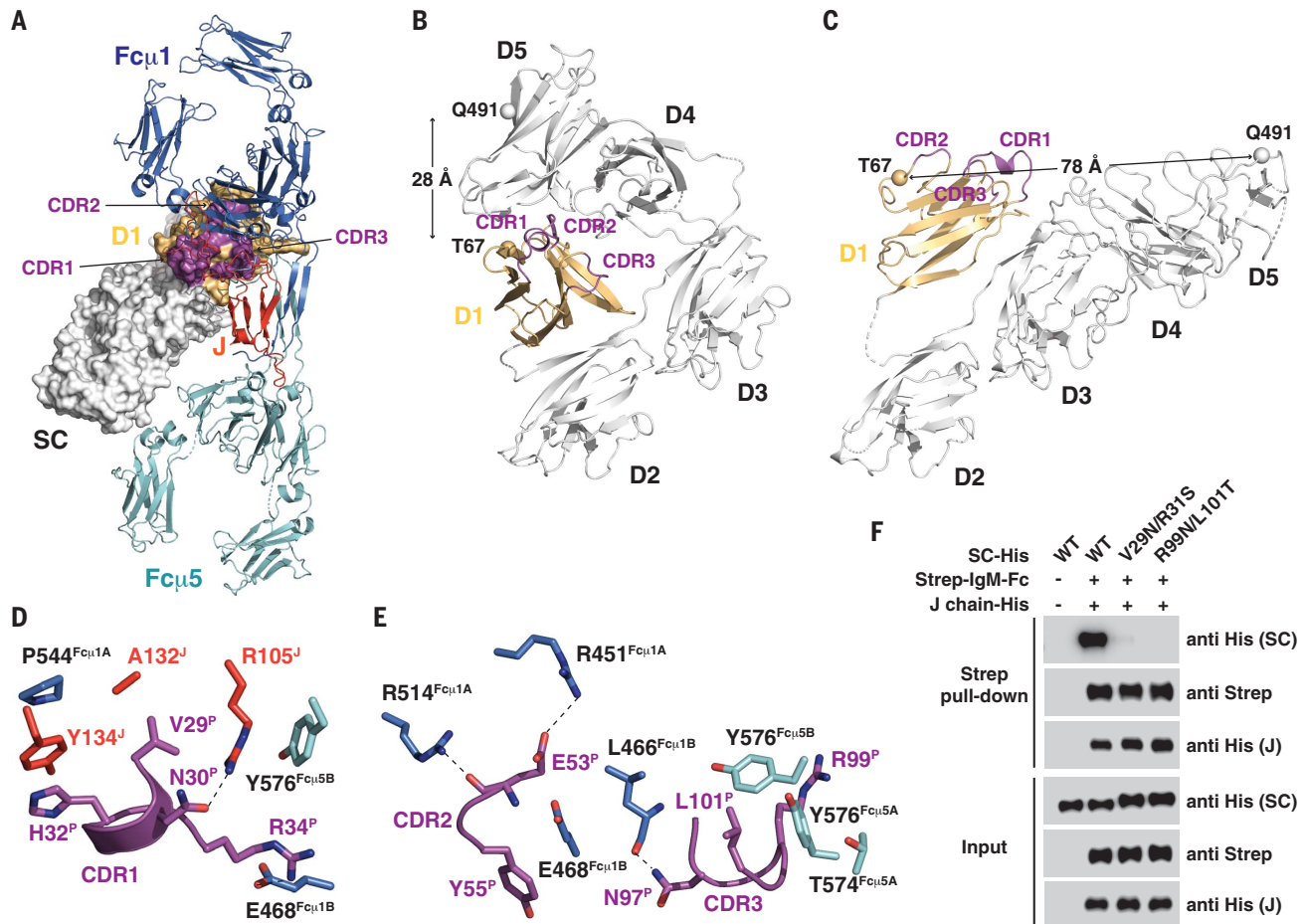


**Fig. 4. Conformational change of pIgR/SC and its interaction with the Fc $\mu$ -J complex.** (A) The three CDRs (magenta) in pIgR/SC-D1 (gold) interact with Fc $\mu$ 1 (blue), Fc $\mu$ 5 (cyan), and the J-chain (red). pIgR/SC is shown as a surface representation. Its D2 to D5 domains are shown in white. (B) The structure of apo pIgR/SC (PDB ID 5D4K). D1 is shown in gold, with the three CDR loops highlighted in magenta. The C $\alpha$  atoms of D1-Thr<sup>67</sup>

and D5-Gln<sup>491</sup> are shown as spheres, and the distance between them is indicated. (C) The structure of pIgR/SC in the Fc $\mu$ -J-SC complex. (D) Detailed view of the interactions at the D1-CDR1 region. Polar interactions are indicated by dashed lines. (E) Detailed view of the interactions at the CDR2 and CDR3 region. (F) SC mutants display reduced interactions with Fc $\mu$ -J.

J-chain residue Arg<sup>105</sup>, which in turn packs onto Tyr<sup>576</sup> of Fc $\mu$ 5B. pIgR/SC residue His<sup>32</sup> packs against J-chain residue Tyr<sup>134</sup>, which interacts with Pro<sup>544</sup> of Fc $\mu$ 1A as described above. pIgR/SC residue Arg<sup>34</sup> forms a salt bridge with Glu<sup>468</sup> of Fc $\mu$ 1B. In CDR2 and CDR3, pIgR/SC residue Glu<sup>53</sup> interacts with both Arg<sup>451</sup> and Arg<sup>514</sup> of Fc $\mu$ 1A (Fig. 4E). It has been reported that rabbit and rodent pIgR can transport IgA but not IgM (23, 24). Rabbit pIgR lacks a residue entirely at this position, whereas rodents feature an Asn (4, 2I). Arg<sup>451</sup> and Arg<sup>514</sup> are also not conserved in mouse IgM (fig. S5A). pIgR/SC residue Tyr<sup>55</sup> packs against Glu<sup>468</sup> of Fc $\mu$ 1B. pIgR/SC residue Asn<sup>97</sup> interacts with the main-chain carbonyl group of Leu<sup>466</sup> of Fc $\mu$ 1B. pIgR/SC residue Arg<sup>99</sup> is sandwiched between Tyr<sup>576</sup> of Fc $\mu$ 5B and Thr<sup>574</sup> of Fc $\mu$ 5A. pIgR/SC residue Leu<sup>101</sup> interacts with Tyr<sup>576</sup> of Fc $\mu$ 5A and Tyr<sup>576</sup> of Fc $\mu$ 5B. Two SC mutants, V29N/R31S and R99N/L101T, which are designed to introduce bulky N-linked glycans in the CDR1 and CDR3 regions, respectively, display greatly reduced interactions with the Fc $\mu$ -J complex (Fig. 4F), confirming the functional relevance of the molecular interactions described above.

Two other IgM receptors exist in mammals in addition to pIgR: Fc $\alpha$  $\mu$ R and Fc $\mu$ R/Toso/Faim3 (25). They each contain a domain that is homologous to the D1 domain of pIgR. Like pIgR, Fc $\alpha$  $\mu$ R binds both IgA and IgM. Its D1-like domain also shows high sequence similarity to pIgR-D1 (fig. S5B), and residues corresponding to pIgR/SC residues Val<sup>29</sup>, Asn<sup>30</sup>, His<sup>32</sup>, Arg<sup>34</sup>, Tyr<sup>55</sup>, and Leu<sup>101</sup> that are involved in binding to the Fc $\mu$ -J complex in pIgR are all present. Thus, Fc $\alpha$  $\mu$ R may interact with IgM in a manner similar to pIgR. Fc $\mu$ R/Toso/Faim3, on the other hand, binds only to IgM. Furthermore, it can interact with both pentameric and hexameric IgM with similar affinities (26).

This is in contrast to pIgR, which selectively binds to the IgM pentamer that contains the J-chain. Indeed, the D1-like domain of Fc $\mu$ R/Toso/Faim3 is more divergent than pIgR-D1 and lacks most of the critical Fc $\mu$ -J-interacting residues (fig. S5C). Thus, Fc $\mu$ R likely binds IgM in a different fashion.

Our high-resolution cryo-EM structure of the Fc $\mu$ -J-SC complex provides a framework for further understanding the functions of IgM, and also sheds light on the interaction between IgM and other receptors. As a result of the stronger binding of IgM to its targets and its more potent activity to induce complement-dependent cytotoxicity, IgM can be potentially exploited for therapeutic applications. Our results pave the way for structure-based engineering of these molecules.

#### REFERENCES AND NOTES

1. I. N. Norderhaug, F. E. Johansen, H. Schjerven, P. Brandtzaeg, *Crit. Rev. Immunol.* **19**, 481–508 (1999).
2. F. E. Johansen, R. Braathen, P. Brandtzaeg, *Scand. J. Immunol.* **52**, 240–248 (2000).
3. J. M. Woof, J. Mestecky, *Immunol. Rev.* **206**, 64–82 (2005).
4. C. S. Kaetzel, *Immunol. Rev.* **206**, 83–99 (2005).
5. H. Turula, C. E. Wobus, *Viruses* **10**, 237 (2018).
6. R. Müller *et al.*, *Proc. Natl. Acad. Sci. U.S.A.* **110**, 10183–10188 (2013).
7. D. M. Czajkowsky, Z. Shao, *Proc. Natl. Acad. Sci. U.S.A.* **106**, 14960–14965 (2009).
8. A. Feinstein, E. A. Munn, *Nature* **224**, 1307–1309 (1969).
9. E. Hiramoto *et al.*, *Sci. Adv.* **4**, eaau1199 (2018).
10. T. H. Sharp *et al.*, *Proc. Natl. Acad. Sci. U.S.A.* **116**, 11900–11905 (2019).
11. F. W. Putnam, G. Florent, C. Paul, T. Shinoda, A. Shimizu, *Science* **182**, 287–291 (1973).
12. D. Eisenberg, M. Jucker, *Cell* **148**, 1188–1203 (2012).
13. D. Pasalic *et al.*, *Proc. Natl. Acad. Sci. U.S.A.* **114**, E8575–E8584 (2017).
14. R. Sitia *et al.*, *Cell* **60**, 781–790 (1990).
15. M. S. Halpern, M. E. Koshland, *Nature* **228**, 1276–1278 (1970).
16. J. Mestecky, J. Zikan, W. T. Butler, *Science* **171**, 1163–1165 (1971).
17. S. Frutiger, G. J. Hughes, N. Paquet, R. Lüthy, J. C. Jaton, *Biochemistry* **31**, 12643–12647 (1992).

18. P. Brandtzaeg, H. Prydz, *Nature* **311**, 71–73 (1984).
19. S. Frutiger, G. J. Hughes, W. C. Hanly, M. Kingzette, J. C. Jaton, *J. Biol. Chem.* **261**, 16673–16681 (1986).
20. R. S. Coyne, M. Siebrecht, M. C. Peitsch, J. E. Casanova, *J. Biol. Chem.* **269**, 31620–31625 (1994).
21. A. E. Hamburger, A. P. West Jr., P. J. Bjorkman, *Structure* **12**, 1925–1935 (2004).
22. B. M. Stadtmueller *et al.*, *eLife* **5**, e10640 (2016).
23. B. J. Underdown, I. Switzer, G. D. Jackson, *J. Immunol.* **149**, 487–491 (1992).
24. M. Røe, I. N. Norderhaug, P. Brandtzaeg, F. E. Johansen, *J. Immunol.* **162**, 6046–6052 (1999).
25. S. Akula, L. Hellman, *Curr. Top. Microbiol. Immunol.* **408**, 1–23 (2017).
26. H. Kubagawa *et al.*, *Curr. Top. Microbiol. Immunol.* **408**, 25–45 (2017).

#### ACKNOWLEDGMENTS

We thank the Core Facilities at the School of Life Sciences, Peking University for help with negative-staining EM; the Cryo-EM Platform of Peking University for help with data collection; the High-Performance Computing Platform of Peking University for help with computation; the National Center for Protein Sciences at Peking University for assistance with Amersham Imager; and G. Li for help with cDNA library. **Funding:** Supported by the National Key Research and Development Program of China (2017YFA0505200 to J.X.; 2016YFC0906000 to J.X. and X.-D.S.; 2019YFA0508904 to N.G.), the National Science Foundation of China (31570735, 31822014 to J.X.; 31725007, 31630087 to N.G.; 21727806 to X.-D.S.; 31922036 to N.L.), the Qidong-SLS Innovation Fund to J.X. and N.G.; and the Clinical Medicine Plus X Project of Peking University to J.X. and Y.T. **Author contributions:** Y.L. performed protein purification; Y.L. and G.W. prepared the cryo-EM sample and collected data; G.W. and N.L. processed the cryo-EM data; J.X. and N.G. built the structural model; Y.L. performed the pull-down experiments; J.X. wrote the manuscript, with inputs from all authors. **Competing interests:** The authors declare no competing financial interests. **Data and materials availability:** The cryo-EM map and atomic coordinates of the Fc $\mu$ -J-SC complex have been deposited in the EMDB and PDB with accession codes EMD-0782 and 6KXS, respectively. All constructs used for protein expression in this study are available upon request.

#### SUPPLEMENTARY MATERIALS

science.sciencemag.org/content/367/6481/1014/suppl/DC1  
Materials and Methods  
Figs. S1 to S5  
Table S1  
References (27–36)

18 September 2019; accepted 24 January 2020  
Published online 6 February 2020  
10.1126/science.aaz5425

## Structural insights into immunoglobulin M

Yaxin Li, Guopeng Wang, Ningning Li, Yuxin Wang, Qinyu Zhu, Huarui Chu, Wenjun Wu, Ying Tan, Feng Yu, Xiao-Dong Su, Ning Gao and Junyu Xiao

*Science* **367** (6481), 1014-1017.

DOI: 10.1126/science.aaz5425 originally published online February 6, 2020

### Hefty structures of IgA and IgM complexes

Immunoglobulin M (IgM) and IgA are antibody isotypes that can form higher-order secretory complexes (sIgM and sIgA), which allows them to effectively bind and neutralize antigens with low-affinity repetitive epitopes, such as those found on the surface of many bacteria and viruses. The assembly and transport of these molecules is also dependent on the joining chain (J-chain) and the polymeric immunoglobulin receptor (pIgR) secretory component (SC). The architecture of these complex, multimeric structures has remained elusive. Li *et al.* resolved cryo-electron microscopy structures of the sIgM-Fc pentamer in complex with the J-chain and SC. Using similar techniques, Kumar *et al.* visualized dimeric, tetrameric, and pentameric structures of secretory sIgA-Fc interacting with the J-chain and SC. Both groups report highly similar mechanisms wherein the J-chain serves as a template for antibody oligomerization. An unanticipated, amyloid-like assembly of the oligomerized structure is present in both cases, with the J-chain conferring asymmetry for pIgR binding and transcytosis. These studies may inform structure-based engineering of these molecules for future therapeutic purposes.

*Science*, this issue p. 1014, p. 1008

#### ARTICLE TOOLS

<http://science.sciencemag.org/content/367/6481/1014>

#### SUPPLEMENTARY MATERIALS

<http://science.sciencemag.org/content/suppl/2020/02/05/science.aaz5425.DC1>

#### REFERENCES

This article cites 36 articles, 11 of which you can access for free  
<http://science.sciencemag.org/content/367/6481/1014#BIBL>

#### PERMISSIONS

<http://www.sciencemag.org/help/reprints-and-permissions>

Use of this article is subject to the [Terms of Service](#)

---

*Science* (print ISSN 0036-8075; online ISSN 1095-9203) is published by the American Association for the Advancement of Science, 1200 New York Avenue NW, Washington, DC 20005. The title *Science* is a registered trademark of AAAS.

Copyright © 2020 The Authors, some rights reserved; exclusive licensee American Association for the Advancement of Science. No claim to original U.S. Government Works